



Acid-catalyzed rearrangements in arenes: interconversions in the quaterphenyl series

Sarah L. Skraba-Joiner, Carter J. Holt and Richard P. Johnson*

Full Research Paper

Open Access

Address:
Department of Chemistry and Materials Science Program, University
of New Hampshire, Durham, NH 03824, USA

Email:
Richard P. Johnson* - Richard.Johnson@unh.edu

* Corresponding author

Keywords:
arenium ion; carbocation; density functional theory; microwave
reaction; rearrangement; superacid

Beilstein J. Org. Chem. **2019**, *15*, 2655–2663.
doi:10.3762/bjoc.15.258

Received: 20 June 2019
Accepted: 18 October 2019
Published: 06 November 2019

This article is part of the thematic issue "Reactive intermediates –
carbocations".

Guest Editor: S. R. Hare

© 2019 Skraba-Joiner et al.; licensee Beilstein-Institut.
License and terms: see end of document.

Abstract

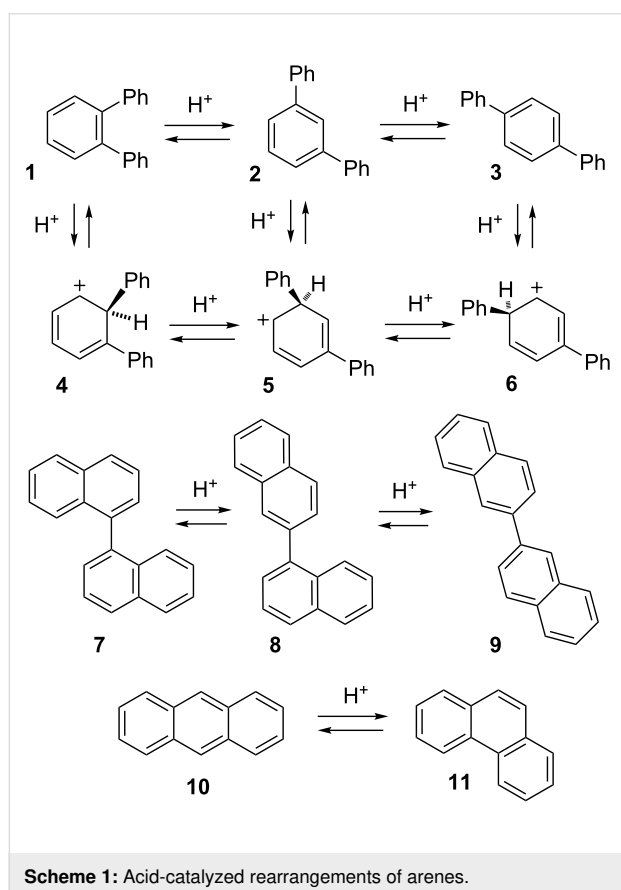
Arenes undergo rearrangement of phenyl, alkyl, halogen and other groups through the intermediacy of *ipso* arenium ions in which a proton is attached at the same carbon as the migrating substituent. Interconversions among the six quaterphenyl isomers have been studied here as a model for rearrangements of linear polyphenyls. All reactions were carried out in 1 M CF₃SO₃H (TfOH) in dichloroethane at 150 °C in a microwave reactor for 30–60 min, with product formation assessed by high field NMR analysis. Under these reaction conditions, *m,p'*-quaterphenyl is the equilibrium product. This isomer is unchanged by the reaction conditions and all other quaterphenyl isomers rearrange to *m,p'* as the dominant or sole product. DFT computations with inclusion of implicit solvation support a complex network of phenyl and biphenyl shifts, with barriers to rearrangement in the range of 10–21 kcal/mol. Consistent with experiments, the lowest energy arenium ion located on this surface is due to protonation of *m,p'*-quaterphenyl. This supports thermodynamic control based on carbocation energies.

Introduction

Carbocations are enigmatic reactive intermediates of enduring importance in chemistry. No other reactive species displays such a complex and fascinating collection of molecular rearrangements. Building on a long history, new synthetic applications [1,2] and explanations of carbocation reaction mechanisms [3-6] continue to be discovered. Chemistry in superacid solutions has played a major role in this field [7,8].

Every student of organic chemistry is taught the importance of arenium ions in the classic two step S_EAr mechanism for electrophilic aromatic substitution. Addition of an electrophile to an arene leads to a bound species, sometimes called a σ -complex, which then loses a proton at the site of substitution to yield the product [9]. Of course challenges to this simple mechanism exist [10-15], including the recent proposal of a one-step

process [16]. Reaction dynamics of electrophile–arene π complexes may also play a role in site selectivity [17]. It is less commonly known that arenium ions, like many other types of carbocations, often rearrange by 1,2-shifts. This leads to a fascinating collection of rearrangements that can migrate hydrogen, halogens or more complex substituents around the ring and even modify the carbon skeleton. Early reports by Baddeley [18] helped to explain odd results from Friedel–Crafts reactions [19] and this type of process is sometime referred to as a Baddeley rearrangement. Many examples of alkyl group migration have been described [19]. Phenyl groups migrate easily and degenerate phenyl shifts in biphenyl were confirmed by isotopic labeling [20,21]. One classic example of arenium ion chemistry is the interconversion of terphenyl isomers **1–3** (Scheme 1). This rearrangement was first reported by Allen and Pingert in 1942 [22] and then independently rediscovered by Olah and Meyer twenty years later [23]. Interconversion of isomers **1–3** is believed to occur through the intermediacy of *ipso* arenium ions **4–6** which connect through 1,2-phenyl shifts.



The term "*ipso*" was first proposed by Perrin and Skinner to explain unusual results in electrophilic substitution reactions; this refers to protonation at the site of a substituent [24]. *Ips*o protonation is the essential step in arenium ion rearrangements.

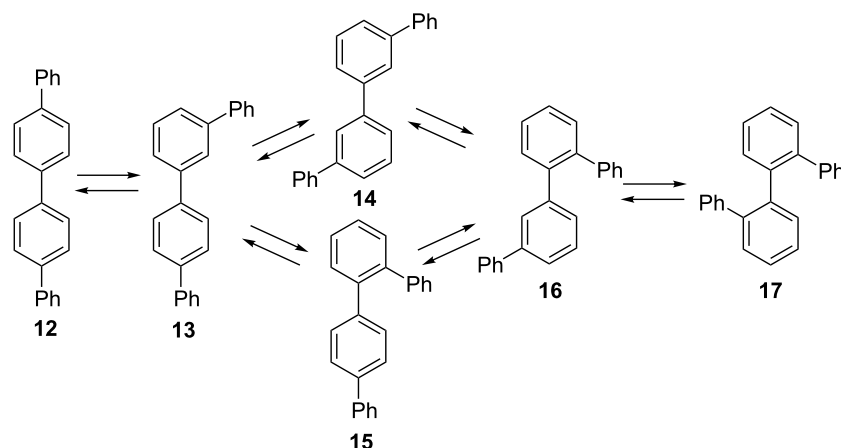
Our interest in this field arose from an accidental rediscovery of rearrangements in the terphenyl series (**1–3**; Scheme 1), by heating **1** with AlCl_3 – a reaction independently discovered twice before [22,23]! We confirmed earlier observations of facile acid-catalyzed interconversion, as well as the fact that *m*-terphenyl (**2**) is favored at equilibrium (observed ratio **1:2:3** is <1:69:31) and used theory to explain this product selectivity [25]. This preference is consistent with formation of the most stable arenium ion intermediate, as shown by DFT computations.

Early studies in this field used AlCl_3 as catalyst and it was generally assumed that adventitious traces of water generated the actual catalyst, precise identity unknown. We found these "water-promoted" reactions with catalytic AlCl_3 to be unreliable. To remove ambiguity about the catalyst and extend the temperature range, we developed a more reliable method for studying higher temperature carbocation rearrangements. In our method, we use 1 M (ca. 20% by volume) trifluoromethanesulfonic acid (TfOH) as catalyst with dichloroethane as our preferred solvent. Most importantly, reactions are conducted in the capped tube of a microwave reactor. With this approach, we can safely and reproducibly heat reactions to ca. 170 °C, so far without incident.

Other more complex rearrangements are easily observed. In the binaphthyl series **7–9**, three sequential rearrangements occur at ambient temperature favoring the 2,2'-isomer **9** (97%) at equilibrium [26]. Aryl shifts occur readily in naphthalene, with beta-substitution favored at equilibrium. Skeletal rearrangements of fused arene rings are also possible and can proceed through several mechanisms. The first example was reported by Dansi and Salvioni in 1941 in the rearrangement of benz[*a*]anthracene to chrysene [27]. We recently studied the rearrangement of anthracene (**10**) to phenanthrene (**11**) [28], finding evidence to support a complex process, suggested earlier [29], that involves initial reduction to 1,2,3,4-tetrahydroanthracene, followed by a pirouette rearrangement of the reduced ring through a spirocyclic intermediate and then re-oxidation to phenanthrene. These reactions involve a complex series of proton and hydride transfers.

Results and Discussion

Beyond terphenyls, acid-catalyzed rearrangements pose limitations in the synthesis of extended polyphenyls but the factors controlling interconversion of isomers are poorly understood [30–33]. As one recent example, Jasti and co-workers showed that cycloparaphenylenes undergo rapid acid-catalyzed rearrangement which precludes using Scholl-type chemistry in this series [30]. In the present work, we have explored rearrangements of quaterphenyls, the next homolog in the paraphenylene



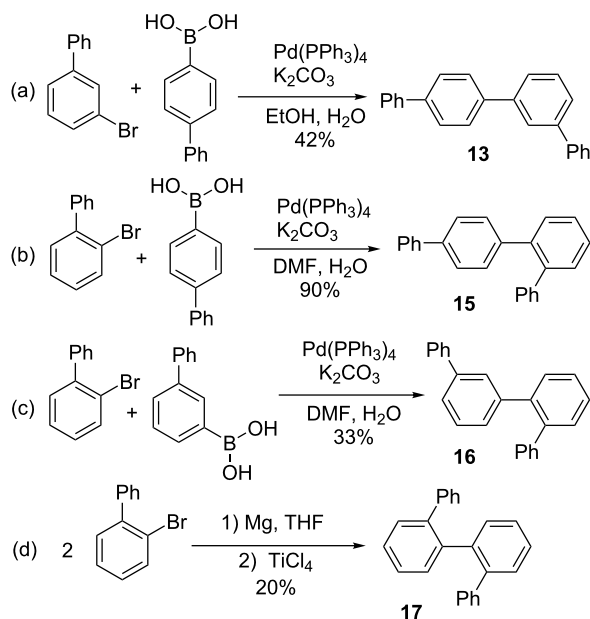
Scheme 2: Rearrangement of quaterphenyl isomers by phenyl shifts.

series, now with six structural isomers. Scheme 2 summarizes interconnections via 1,2-migration of a terminal phenyl group. As will be shown below, an internal aryl–aryl bond can also be transposed through 1,2-biphenyl migration, with a similar network of interconversions. Based on the behavior of terphenyl which favors *meta* substitution at equilibrium, we initially hypothesized that *m,m'*-quaterphenyl (**14**) would likely be the major isomer at equilibrium.

Only brief exploration of quaterphenyl rearrangements had been described previously. Isomerization of *o,o'*-quaterphenyl (**17**) with $\text{SnCl}_4/\text{AlCl}_3$ catalysis has been reported to yield a mixture of *p,p'*- (**12**), *m,p'*- (**13**), and *m,m'*-quaterphenyl (**14**) [34].

p,p'-Quaterphenyl (**12**) and *m,m'*-quaterphenyl (**14**) were available commercially. To complete the series, samples of *m,p'*- (**13**), *o,p'*- (**15**), *o,m'*- (**16**), and *o,o'*-quaterphenyl (**17**) were synthesized as shown in Scheme 3. Suzuki–Miyaura coupling was used to synthesize **13**, **15**, and **16** from the corresponding aryl bromides and boronic acids [35]. *o,o'*-Quaterphenyl (**17**) was synthesized by homo-coupling of 2-bromobiphenyl, as previously reported [36].

Promoting the rearrangement of all quaterphenyl isomers at room temperature or in refluxing DCE (84 °C) proved to be difficult because *p,p'*-quaterphenyl (**12**) is very poorly soluble in this solvent and higher temperatures were required in some cases to reach equilibrium. In a solution of 1 M TfOH/DCE, **12** forms a colored solution more slowly (ca. 1–2 min) than previous examples we have studied. Heating these reaction mixtures in a microwave reactor allows for the substrate to dissolve in the reaction medium, resulting in a rearrangement. To provide a consistent reaction environment, the rearrangement of all isomers was studied using a microwave reactor at 150 °C,



Scheme 3: Synthesis of quaterphenyl isomers.

with reaction times of 30 or 60 min. After chromatographic purification to remove oligomeric material, product distributions were determined by high field ^1H NMR, with integration of unique resonances for each isomer. In these reactions, we attribute no special effect due to microwaves. This has been a subject of some debate in the literature [37,38]. As we have demonstrated earlier, the microwave reactor simply provides a safe and reliable way to heat samples with superacids at temperatures well above the normal solvent boiling point.

The results of quaterphenyl isomerizations are summarized in Table 1. Initially it was expected that *m,m'*-quaterphenyl (**14**)

Table 1: Product distributions from rearrangement of quaterphenyl isomers.^{a,b}

Reactant	Time (min)	12	13	14	15	16	17	Yield
12	30	–	100	–	–	–	–	70
12	60	–	100	–	–	–	–	55
13	30	–	100	–	–	–	–	88
13	60	–	100	–	–	–	–	75
14	30	–	50	50	–	–	–	81
14	60	–	67	33	–	–	–	90
15	30	–	81	19	–	–	–	70
16	30	–	57	43	–	–	–	64
17	30	–	60	40	–	–	–	67

^aAll reactions were carried out in 1 M CF₃SO₃H in dichloroethane at 150 °C in a microwave reactor. ^bYields are total isolated products after flash chromatography.

might be the major isomer formed at equilibrium, as previous examples have heavily favored *meta*-substitution patterns. Contrary to this expectation, the major product observed in all cases was *m,p'*-quaterphenyl (**13**). In 30 min at 150 °C, *p,p'*-quaterphenyl (**12**) isomerized completely to **13**. Under the same conditions, *m,m'*-quaterphenyl (**14**) isomerized more slowly, yielding **13** and **14** in a 50:50 mixture in 30 min. Increased reaction time with *m,m'*-quaterphenyl (**14**) yielded **13** and **14** in a 67:33 ratio. Starting with *o,m'*- (**16**) or *o,o'*-quaterphenyl (**17**) yielded a mixture of ca. 60% **13** and ca. 40% **14** in 30 min. Similarly, *o,p'*-quaterphenyl (**15**) isomerized to an 81:19 mixture of **13**:**14**. When starting with *m,p'*-quaterphenyl, no rearrangement to **14** was observed, even at increased reaction times.

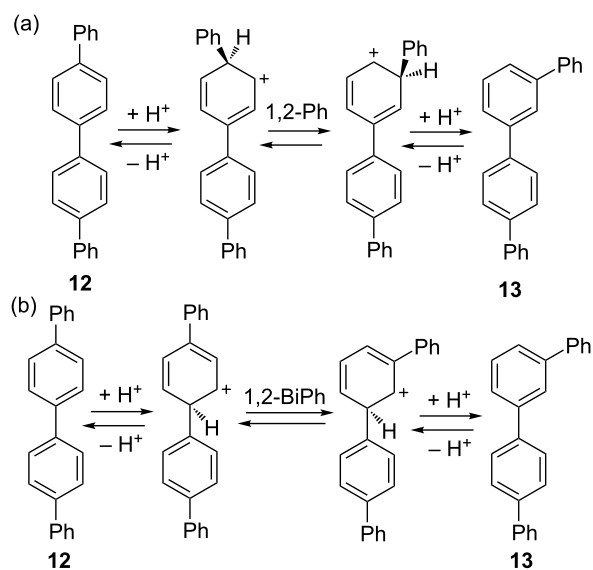
Minor products with more downfield chemical shifts were also observed *via* ¹H NMR of these crude product mixtures; these were easily separated from quaterphenyl isomers using flash column chromatography. Analysis of the crude product mixtures by MALDI-TOF-MS confirmed these minor products could be attributed to oligomerization (*m/z* = 344, 673).

Our conclusion from this series of experiments is that *m,p'*-quaterphenyl (**13**) is the equilibrium product from rearrangement of all of the six isomers. This is most clearly demonstrated in the rearrangement of **12** to **13** and the failure of **13** to produce other isomers. In some cases, reaction times were insufficient to fully reach equilibrium.

Computational models for quaterphenyl rearrangements

While the energy surface for the interconversion of quaterphenyl isomers initially seems straightforward, there are additional modes of rearrangement that must be considered. 1,2-Phenyl shifts are possible to interconvert isomers, occurring through protonation at the *ipso* site on the external phenyl rings

(Scheme 4a). Biphenyl shifts are also possible through protonation at the internal *ipso* sites (Scheme 4b). This results in a very complex potential energy surface. Protonation of a terminal phenyl group can also lead to terphenyl migration but this process is structurally degenerate and was not explored by computations.



Scheme 4: Rearrangement of quaterphenyl isomers via (a) 1,2-phenyl shift and (b) 1,2-biphenyl shift.

Both phenyl and biphenyl rearrangement pathways were studied by DFT methods, with inclusion of implicit solvation by the polarizable continuum model (PCM). As in our earlier research, we employed B3LYP/6-31+G(d,p) theory with PCM solvation in dichloroethane [25,26,28]. As noted earlier by Tantillo, the B3LYP functional provides a very good description of carbocation chemistry [3].

Figure 1 shows the lowest energy pathways for 1,2-phenyl shifts, while Figure 2 shows those for a 1,2-biphenyl shifts. In each case, the energy reference is arbitrarily chosen as the linear *ipso* cation **12c** or **12d** for phenyl or biphenyl shift, respectively. Predicted barriers for rearrangements of *ipso* cations are all in the range of 9–22 kcal/mol. Common to both potential energy surfaces are the lowest energy non-*ipso* carbocations **12a–17a** which lie at the bottom on the energy scale. It is noteworthy that *m,p'* cation **13a** is the lowest energy species predicted by our calculations. In each diagram, double-headed vertical arrows show the energy difference between *ipso* cations and their non-*ipso* counterpart which might be formed rapidly by secondary 1,2-hydride shifts.

In principle, the equilibrium product in these complex reactions might correlate with relative energies of the neutral quaterphenyl isomers. Reliable heats of formation for quaterphenyls are unavailable in the literature but these values and other estimates for relative energies can be predicted by theory. Starting with the lowest energy conformer for each quaterphenyl, we first computed heats of formation using the T1 method [39]. Predicted values (Supporting Information File 1) are narrowly clustered in a range of ca. 2 kcal/mol, with the lowest energy isomer predicted to be *o,o'*-quaterphenyl (**17**). This low ranking for the most congested isomer may be attributed to intramolecu-

lar π stacking. Very similar results were obtained with M06-2X/6-311+G(d,p) theory, which also placed **17** as the lowest energy quaterphenyl isomer. Our results thus do not support thermodynamic control based on relative energies of the neutral quaterphenyls.

A more plausible scenario is that thermodynamic control applies to carbocation intermediates, with the equilibrium product determined by the energy of the lowest energy carbocation in solution. This is predicted to be **13a**. The speed of equilibration for different isomers is determined by the number of required steps and their barriers. Thus **12** rearranges to **13** in a phenyl or biphenyl migration, passing through **TS7** or **TS13**, respectively. This rearrangement is complete in our standard 30 min reaction time. By contrast, **17** requires three separate migration steps to arrive at **13**, passing through **16** and **14**; this rearrangement (Table 1) is incomplete during the same reaction period.

An unknown factor is the degree of protonation, especially at 150 °C. We observed earlier by NMR spectroscopy that anthracene is fully protonated at ambient temperature in 1M TfOH but 1,3,5-triphenylbenzene is not [28]. One experimental observation is that the 1M TfOH/arene reaction solutions invariably have a bright color at ambient temperature due to the

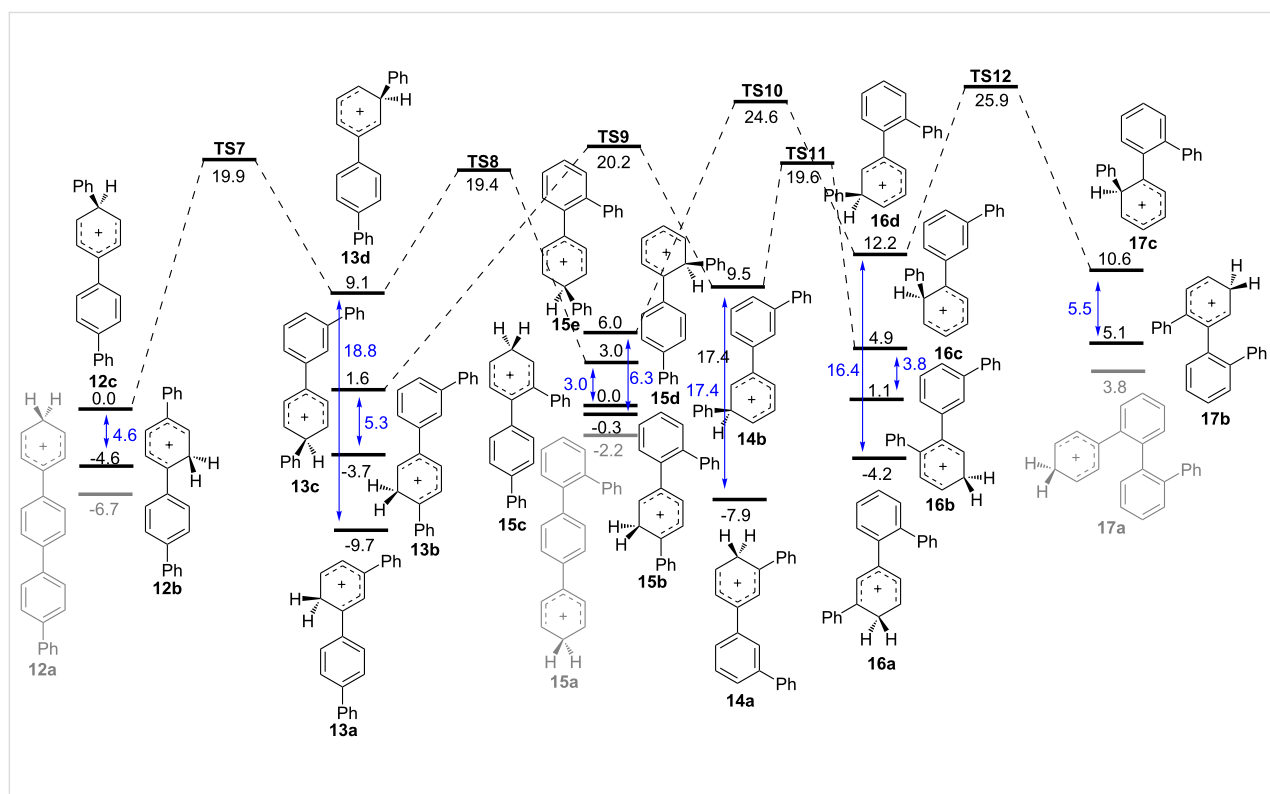


Figure 1: Pathways for terminal 1,2-phenyl shifts in quaterphenyl isomers calculated with IEFPCM(DCE)/B3LYP/6-31+G(d,p) theory. Relative free energies are given in kcal/mol.

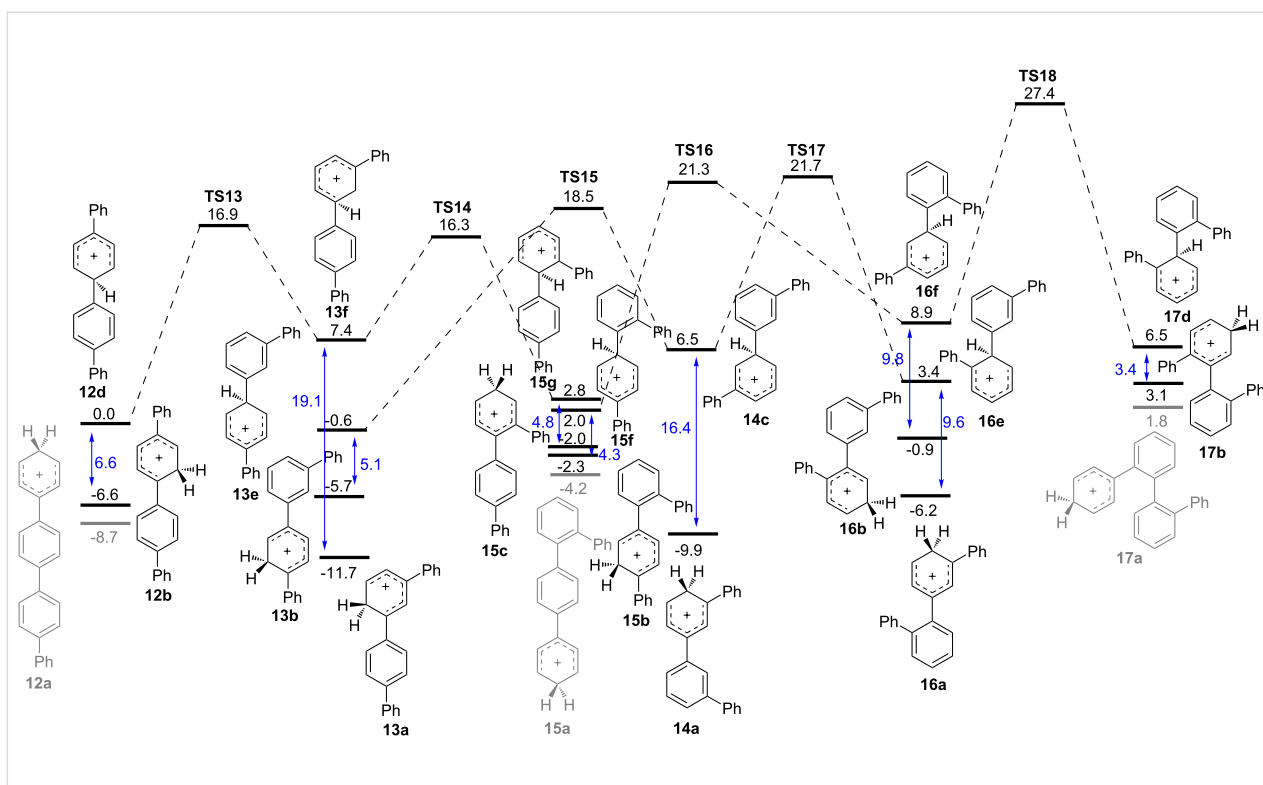
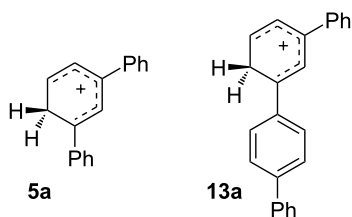


Figure 2: Pathways for 1,2-biphenyl shifts in quaterphenyl isomers calculated with IEFPCM(DCE)/B3LYP/6-31+G(d,p) theory. Relative free energies are given in kcal/mol.

carbocation [40,41]. As these solutions are heated, they become much darker in color, implying a higher level of protonation. Upon cooling, a more normal color is returned. Full protonation of **13** at 150 °C would explain thermodynamic control by cationic intermediates.

Our naïve supposition at the outset of this project that *m,m'*-quaterphenyl **14** might be favored at equilibrium was unsupported by experiment, which instead showed the *m,p'* isomer **13** to be preferred. A comparison of **5a**, the lowest energy cation from terphenyl rearrangements, with **13a**, the corresponding cation for quaterphenyls, provides a simple explanation. If a single ring is protonated, greater stability accrues from a *para* phenyl substituent with *meta* a close second. The same effect should apply to longer polyphenylene chains, resulting in a chain of aryl groups that remains mostly *para* after generating a more basic *meta* substituted site.



Conclusion

Acid-catalyzed interconversions among the six quaterphenyl isomers have been studied in this work as a model for rearrangements of linear polyphenyls. All reactions were carried out in 1 M CF₃SO₃H (TfOH) in dichloroethane at 150 °C in a microwave reactor for 30 or 60 min, with product formation assessed by high field NMR analysis. Under these reaction conditions, *m,p'*-quaterphenyl (**13**) is the equilibrium product. This isomer is unchanged by the reaction conditions and all other quaterphenyl isomers rearrange to *m,p'* as the dominant or sole product. DFT computations with inclusion of implicit solvation support a complex network of phenyl and biphenyl shifts, with barriers to rearrangement in the range of 10–21 kcal/mol. Consistent with experiments, the lowest energy arenium ion located on this surface is due to protonation of *m,p'*-quaterphenyl. This supports thermodynamic control based on carbocation energies. The same effect may apply to longer polyphenylene chains, resulting in a chain of aryl groups that does not fully rearrange but remains mostly *para* after generating a more basic *meta* substituted site.

Experimental

General methods. Trifluoromethanesulfonic acid (TfOH, 99% purity) and dichloroethane (DCE, 99+%) were used as received from commercial sources. Glassware was oven dried

and all reactions were run under a nitrogen atmosphere. ^1H NMR spectra were measured in CDCl_3 using a Varian XL-400 MHz spectrometer. Microwave reactions were conducted using a single-mode CEM microwave reactor in 10 mL vessels with temperature monitoring by an external sensor.

General procedure for rearrangement in the microwave (MW) reactor. In a similar manner as described in [28], under a nitrogen atmosphere, the substrate (ca. 4–50 mg) and 1,2-dichloroethane (DCE, 4 mL) were added to a 10 mL reaction vessel. Trifluoromethanesulfonic acid (TfOH) (0.40 mL, 4.5 mmol) was added dropwise by syringe; this typically caused formation of a bright color. The reaction mixture was purged with nitrogen, capped and heated in a microwave reactor. Reaction times represent hold times after a ramp time of ca. 10 minutes. After cooling, products were isolated by careful neutralization with saturated aqueous NaHCO_3 and extraction with dichloromethane. The crude product mixture was purified by flash chromatography then analyzed using ^1H NMR. The presence of oligomeric material was assessed on crude isolated product through time-of-flight matrix assisted laser desorption ionization (MALDI-TOF-MS) mass spectrometry, using sulfur as a matrix.

Suzuki–Miyaura coupling to form *m,p'*-quaterphenyl (13) [35]: 4-Biphenylboronic acid (0.18 g, 0.91 mmol) and 1 M K_2CO_3 (1.5 mL) were added to a 10 mL Pyrex microwave tube. 3-Bromobiphenyl (0.07 mL, 0.42 mmol), ethanol (2.3 mL), and $\text{Pd}(\text{PPh}_3)_4$ (28 mg, 0.24 mmol) were then added. The headspace was purged with nitrogen and the tube was capped before the reaction mixture was placed in a microwave reactor (150 °C, 30 min hold time). After the reaction, the mixture was quenched with 1 M NaOH , extracted with dichloromethane, washed with water and brine, and dried with Na_2SO_4 . The organic layer was then concentrated to a brown solid and purified by chromatography with hexanes to yield *m,p'*-quaterphenyl (**13**) as a white solid (0.058 g, mp 163–166 °C, lit 167–168 °C, 42% yield); ^1H NMR (400 MHz, CDCl_3) δ 7.87–7.85 (m, 1H), 7.76–7.69 (m, 4H), 7.69–7.64 (m, 4H), 7.64–7.58 (m, 2H), 7.57–7.52 (m, 1H), 7.50–7.45 (m, 4H), 7.41–7.35 (m, 2H).

Suzuki–Miyaura coupling to form *o,p'*-quaterphenyl (15) [35]: K_2CO_3 (0.91 g, 6.6 mmol) and water (7.7 mL) were combined in a 25 mL round bottom flask which was purged with nitrogen, and cooled to 0 °C. Biphenyl-4-boronic acid (0.89 g, 4.5 mmol) was added, followed by 2-bromobiphenyl (0.50 g, 2.2 mmol), DMF (11.5 mL) and $\text{Pd}(\text{PPh}_3)_4$ (0.13 g, 0.1 mmol). The reaction mixture was stirred at 0 °C for 5 h. NaOH (1 M, 10 mL) was added and the product was extracted

with DCM. The organic extract was washed with water and brine and dried with Na_2SO_4 . The crude product was purified by flash chromatography with hexanes to yield *o,p'*-quaterphenyl as a white solid (0.55 g, mp 107–109 °C, lit 117–120 °C, 90% yield). ^1H NMR (400 MHz, CDCl_3) δ 7.61–7.57 (m, 2H), 7.50–7.40 (m, 8H), 7.35–7.29 (m, 1H), 7.26–7.17 (m, 7H).

Suzuki–Miyaura coupling to form *o,m'*-Quaterphenyl (16) [35]: 2-Bromobiphenyl (0.20 g, 0.80 mmol), biphenyl-3-boronic acid (0.25 g, 1.3 mmol), and $\text{Pd}(\text{PPh}_3)_4$ (0.02 g, 0.02 mmol) were dissolved in DMF (10 mL). The reaction mixture was cooled to 0 °C and purged with nitrogen. A solution of K_2CO_3 (0.20 g, 1.5 mmol) and water (5 mL) was added via syringe and the reaction mixture was stirred at 0 °C for 5 h. The product was extracted with DCM, and washed with water, NaOH , and HCl . The organic extract was then washed with water and brine and dried with Na_2SO_4 . The crude product was purified by flash chromatography with hexanes to yield *o,m'*-quaterphenyl as a white solid (0.085 g, mp 84–86 °C, lit 90–91 °C, 33% yield). ^1H NMR (400 MHz, CDCl_3) δ 7.52–7.47 (m, 1H), 7.47–7.40 (m, 4H), 7.38–7.29 (m, 6H), 7.29–7.26 (m, 1H), 7.26–7.22 (m, 3H), 7.21–7.15 (m, 3H).

Synthesis of *o,o'*-quaterphenyl (17) [36]: A solution of 2-bromobiphenyl (0.15 g, 0.65 mmol), magnesium turnings (0.02 g, 0.69 mmol), and THF (2 mL) was stirred at ambient temperature overnight under a nitrogen atmosphere. Additional THF (4 mL) was added and the reaction mixture was cooled to –78 °C via a dry ice/acetone bath. TiCl_4 (0.14 g, 0.65 mmol) was added dropwise via syringe and the reaction mixture was warmed to 0 °C via an ice/water bath and stirred for 1 h. The product was extracted with ethyl acetate (3x) and dried with Na_2SO_4 . The crude product was purified by chromatography with hexanes to yield *o,o'*-quaterphenyl as a white solid (0.040 g, mp 110–113 °C, lit 116–118 °C, 20% yield). ^1H NMR (400 MHz, CDCl_3) δ 7.4–7.40 (m, 2H), 7.38–7.29 (m, 4H), 7.18–7.14 (m, 2H), 7.10–7.05 (m, 2H), 7.03–6.96 (m, 4H), 6.62–6.59 (m, 4H).

Rearrangement of quaterphenyl isomers in a microwave reactor

***p,p'*-Quaterphenyl (12):** 150 °C, 30 min. Compound **12** (17 mg, 0.06 mmol) was heated in a MW reactor (150 °C, 30 min) according to the general rearrangement procedure. The crude product was purified via CombiFlash with hexanes to yield *m,p'*-quaterphenyl (**13**) as an off-white solid (12 mg, 70% yield).

***m,p'*-Quaterphenyl (13):** 150 °C, 30 min. Compound **13** (17 mg, 0.05 mmol) was heated in a MW reactor (150 °C, 30 minutes) according to the general rearrangement procedure.

The crude product was filtered over a silica plug with hexanes to yield **13** as an off-white solid (15 mg, 88% yield).

150 °C, 1 h. **13** (16 mg, 0.05 mmol) was heated in a MW reactor (150 °C, 1 h) according to the general rearrangement procedure. The crude product was filtered over a silica plug with hexanes to yield **13** as an off-white solid (12 mg, 75% yield).

***m,m'*-Quaterphenyl (14)**: 150 °C, 30 min. Compound **14** (16 mg, 0.05 mmol) was heated in a MW reactor (150 °C, 30 minutes) according to the general rearrangement procedure. The crude product was purified via CombiFlash with hexanes to yield an off-white solid (13 mg, 81% yield) consisting of **13** (50%) and **14** (50%).

150 °C, 1 h. Compound **12** (10 mg, 0.03 mmol) was heated in a MW reactor (150 °C, 1 h) according to the general rearrangement procedure. The crude product was filtered over a silica plug with hexanes to yield an off-white solid (9 mg, 90% yield) consisting of **13** (67%) and **14** (33%).

***o,p'*-Quaterphenyl**: Compound **15** (10 mg, 0.03 mmol) was heated in a MW reactor (150 °C, 30 minutes) according to the general rearrangement procedure. The crude product was purified via CombiFlash with hexanes to yield an off-white solid (7 mg, 70% yield) consisting of **13** (81%) and **14** (19%). Minor products were eluted with ethyl acetate. MALDI–TOF–MS analysis indicated oligomerization ($m/z = 344, 673$).

***o,m'*-Quaterphenyl**: Compound **16** (28 mg, 0.09 mmol) was heated in a MW reactor (150 °C, 30 minutes) according to the general rearrangement procedure. The crude product was filtered over a silica plug with hexanes to yield an off-white solid (18 mg, 64% yield) consisting of **13** (57%) and **14** (43%).

***o,o'*-Quaterphenyl**: Compound **17** (6 mg, 0.02 mmol) was heated in a MW reactor (150 °C, 30 minutes) according to the general rearrangement procedure. The crude product was filtered over a silica plug with hexanes to yield an off-white solid (4 mg, 67% yield) consisting of **13** (60%) and **14** (40%).

Computational methods: DFT computations on carbocation intermediates and transition states were carried out with the B3LYP functional and 6-31+G(d,p) basis set, using the polarizable continuum model in dichloroethane to model solvation [42]. Each stationary point was characterized as a minimum or transition state by vibrational frequency analysis but the large number of reaction paths precluded calculation of intrinsic reaction coordinates. Reported relative energies are from free energy calculations at 298 K.

Supporting Information

Supporting Information File 1

Selected NMR spectra, MALDI spectrum of the product mixture, Cartesian coordinates, and summary energetics for all stationary points.

[<https://www.beilstein-journals.org/bjoc/content/supplementary/1860-5397-15-258-S1.pdf>]

Acknowledgements

We are grateful for support from National Science Foundation award CHE-1362519. This research used the Extreme Science and Engineering Discovery Environment (XSEDE), supported by NSF Grant No. OCI-1053575.

ORCID® iDs

Sarah L. Skraba-Joiner - <https://orcid.org/0000-0002-1545-0608>

Carter J. Holt - <https://orcid.org/0000-0001-7459-353X>

Richard P. Johnson - <https://orcid.org/0000-0002-1100-6235>

References

- Klumpp, D. A. Carbocations. In *Organic Reaction Mechanisms*; Knipe, A. C., Ed.; John Wiley & Sons, Ltd, 2016; pp 273–319. doi:10.1002/9781118707838.ch6
- Naredla, R. R.; Klumpp, D. A. *Chem. Rev. (Washington, DC, U. S.)* **2013**, *113*, 6905–6948. doi:10.1021/cr4001385
- Tantillo, D. J. *Angew. Chem., Int. Ed.* **2017**, *56*, 10040–10045. doi:10.1002/anie.201702363
- Sandbeck, D. J. S.; Markewich, D. J.; East, A. L. L. *J. Org. Chem.* **2016**, *81*, 1410–1415. doi:10.1021/acs.joc.5b02553
- Pontes, R. M. *Theor. Chem. Acc.* **2018**, *137*, 56. doi:10.1007/s00214-018-2232-1
- Hare, S. R.; Tantillo, D. J. *Beilstein J. Org. Chem.* **2016**, *12*, 377–390. doi:10.3762/bjoc.12.41
- Prakash, G. K. S. *J. Org. Chem.* **2006**, *71*, 3661–3676. doi:10.1021/jo052657e
- Olah, G. A. *J. Org. Chem.* **2001**, *66*, 5943–5957. doi:10.1021/jo010438x
- Klumpp, D. A. In *Arene Chemistry*; Mortier, J., Ed.; John Wiley & Sons, Inc: Hoboken, NJ, 2016; pp 3–31.
- Oliveira, F. G.; Rodrigues, F. L.; de Oliveira, A. V. B.; Marçal, D. V. L. M.; Esteves, P. M. *Struct. Chem.* **2017**, *28*, 545–553. doi:10.1007/s11224-017-0915-1
- Chen, Z.; Mo, Y. *J. Chem. Theory Comput.* **2013**, *9*, 4428–4435. doi:10.1021/ct400618k
- Freire de Queiroz, J.; Carneiro, J. W. d. M.; Sabino, A. A.; Sparrapan, R.; Eberlin, M. N.; Esteves, P. M. *J. Org. Chem.* **2006**, *71*, 6192–6203. doi:10.1021/jo0609475
- Esteves, P. M.; Walkimar de Carneiro, J.; Cardoso, S. P.; Barbosa, A. G. H.; Laali, K. K.; Rasul, G.; Prakash, G. K. S.; Olah, G. A. *J. Am. Chem. Soc.* **2003**, *125*, 4836–4849. doi:10.1021/ja021307w
- Rosokha, S. V.; Kochi, J. K. *J. Org. Chem.* **2002**, *67*, 1727–1737. doi:10.1021/jo011072r

15. Kim, E. K.; Bockman, T. M.; Kochi, J. K. *J. Am. Chem. Soc.* **1993**, *115*, 3091–3104. doi:10.1021/ja00061a007
16. Galabov, B.; Nalbantova, D.; Schleyer, P. v. R.; Schaefer, H. F., III. *Acc. Chem. Res.* **2016**, *49*, 1191–1199. doi:10.1021/acs.accounts.6b00120
17. Nieves-Quinones, Y.; Singleton, D. A. *J. Am. Chem. Soc.* **2016**, *138*, 15167–15176. doi:10.1021/jacs.6b07328
18. Baddeley, G.; Kenner, J. *J. Chem. Soc.* **1935**, 303–309. doi:10.1039/jr9350000303
19. Nightingale, D. V. *Chem. Rev.* **1939**, *25*, 329–376. doi:10.1021/cr60082a001
20. Wynberg, H.; Wolf, A. P. *J. Am. Chem. Soc.* **1963**, *85*, 3308. doi:10.1021/ja00903a064
21. Necula, A.; Racoveanu-Schicketanz, A.; Gheorghiu, M. D.; Scott, L. T. *J. Org. Chem.* **1995**, *60*, 3448–3451. doi:10.1021/jo00116a035
22. Allen, C. F. H.; Pingert, F. P. *J. Am. Chem. Soc.* **1942**, *64*, 1365–1371. doi:10.1021/ja01258a038
23. Olah, G. A.; Meyer, M. W. *J. Org. Chem.* **1962**, *27*, 3682–3683. doi:10.1021/jo01057a505
24. Perrin, C. L.; Skinner, G. A. *J. Am. Chem. Soc.* **1971**, *93*, 3389–3394. doi:10.1021/ja00743a015
25. Ajaz, A.; McLaughlin, E. C.; Skraba, S. L.; Thamam, R.; Johnson, R. P. *J. Org. Chem.* **2012**, *77*, 9487–9495. doi:10.1021/jo301848g
26. Skraba-Joiner, S. L.; McLaughlin, E. C.; Ajaz, A.; Thamam, R.; Johnson, R. P. *J. Org. Chem.* **2015**, *80*, 9578–9583. doi:10.1021/acs.joc.5b01559
27. Dansi, A.; Salvioni, E. *Gazz. Chim. Ital.* **1941**, *71*, 549–552.
28. Skraba-Joiner, S. L.; Brulet, J. W.; Song, M. K.; Johnson, R. P. *J. Org. Chem.* **2017**, *82*, 13076–13083. doi:10.1021/acs.joc.7b02058
29. Cook, B. R.; Colgrove, S. G. *Prepr. - Am. Chem. Soc., Div. Pet. Chem.* **1994**, *39*, 372–378.
30. Sisto, T. J.; Zakharov, L. N.; White, B. M.; Jasti, R. *Chem. Sci.* **2016**, *7*, 3681–3688. doi:10.1039/c5sc04218f
31. Ormsby, J. L.; Black, T. D.; Hilton, C. L.; Bharat; King, B. T. *Tetrahedron* **2008**, *64*, 11370–11378. doi:10.1016/j.tet.2008.09.105
32. He, J.; Mathew, S.; Kinney, Z. J.; Warrell, R. M.; Molina, J. S.; Hartley, C. S. *Chem. Commun.* **2015**, *51*, 7245–7248. doi:10.1039/c5cc00826c
33. Mathew, S.; Crandall, L. A.; Ziegler, C. J.; Hartley, C. S. *J. Am. Chem. Soc.* **2014**, *136*, 16666–16675. doi:10.1021/ja509902m
34. Copeland, P. G.; Dean, R. E.; McNeil, D. *J. Chem. Soc.* **1960**, 4522–4524. doi:10.1039/jr9600004522
35. Lima, C. F. R. A. C.; Rodrigues, A. S. M. C.; Silva, V. L. M.; Silva, A. M. S.; Santos, L. M. N. B. F. *ChemCatChem* **2014**, *6*, 1291–1302. doi:10.1002/cctc.201301080
36. King, B. T.; Kroulik, J.; Robertson, C. R.; Rempala, P.; Hilton, C. L.; Korinek, J. D.; Gortari, L. M. *J. Org. Chem.* **2007**, *72*, 2279–2288. doi:10.1021/jo061515x
37. Kappe, C. O.; Pieber, B.; Dallinger, D. *Angew. Chem., Int. Ed.* **2013**, *52*, 1088–1094. doi:10.1002/anie.201204103
38. Dudley, G. B.; Stiegman, A. E. *Chem. Rec.* **2018**, *18*, 381–389. doi:10.1002/tcr.201700044
39. Ohlinger, W. S.; Klunzinger, P. E.; Deppmeier, B. J.; Hehre, W. J. *J. Phys. Chem. A* **2009**, *113*, 2165–2175. doi:10.1021/jp810144q
40. Garkusha, I.; Fulara, J.; Nagy, A.; Maier, J. P. *Astrophys. J.* **2011**, *728*, 131. doi:10.1088/0004-637x/728/2/131
41. Dallinga, G.; Mackor, E. L.; Verrijn Stuart, A. A. *Mol. Phys.* **1958**, *1*, 123–140. doi:10.1080/00268975800100151
42. Tomasi, J.; Mennucci, B.; Cammi, R. *Chem. Rev.* **2005**, *105*, 2999–3093. doi:10.1021/cr9904009

License and Terms

This is an Open Access article under the terms of the Creative Commons Attribution License (<http://creativecommons.org/licenses/by/4.0>). Please note that the reuse, redistribution and reproduction in particular requires that the authors and source are credited.

The license is subject to the *Beilstein Journal of Organic Chemistry* terms and conditions: (<https://www.beilstein-journals.org/bjoc>)

The definitive version of this article is the electronic one which can be found at: <doi:10.3762/bjoc.15.258>